LA-UR-03-2275

*Approved for public release; distribution is unlimited.*

*Title:* Monte Carlo Model for Proton Elastic Scattering from Optical Model Calculations

*Author(s):* R. E. Prael, LANL X-5
Lon-Chang Liu, LANL T-16
Sergei Striganov, FNAL

*Submitted to:* American Nuclear Society Summer Meeting, June1-5, San Diego (Topical Meeting on Accelerator Applications)

# Monte Carlo Model for Proton Elastic Scattering from Optical Model Calculations


R. E. Prael* and Lon-Chang Liu

*Los Alamos National Laboratory*
*Los Alamos, NM 87545*

and

Sergei Striganov†

*Fermi National Accelerator Laboratory*
*Batavia, IL 60510*



**Abstract**–*A Monte Carlo elastic scattering method for protons has been developed for application to proton radiography at high energies. The method uses a processed data library derived from optical model calculations for 22 nuclei* $2 \leq \mathrm{A} \leq 242$ *and 47 lab momenta over the range* $1\ \mathrm{GeV/c} \leq \mathrm{P_{lab}} \leq 50\ \mathrm{GeV/c}$. *The proton-nucleus elastic differential cross sections were calculated in the framework of eikonal theory. At the present stage, we have only used the first-order optical potential which is a convolution between the proton-nucleon scattering amplitudes (*$f_{pp}$, $f_{pn}$*) and the nuclear matter density. Without any free parameter, the calculated differential cross sections describe well the existing data, indicating that effects of higher-order optical potential can be expected to be small. For each mass and energy in the data library, the original cross section calculations are represented as a sampling distribution for the dimensionless variable* $X$ *where* $X = q/q_1 = 2p\sin(\theta/2)/q_1$ *for center of mass momentum* $p$, *momentum transfer* $q$ *and scattering angle* $\theta$. *The variable* $q_1$ *is the momentum transfer at the first diffraction minimum. The method accurately reproduces the original optical model calculations over a range of* $10^7$ *in cross section. The representation, which separates the sampling distribution for* $X$ *from the mass and energy dependence of the scattering cross section and* $q_1$, *provides good interpolation properties over intermediate masses and energies.*


## I. INTRODUCTION

A Monte Carlo elastic scattering method for protons has been developed for application to proton radiography[1] at high energies. It addresses one process leading to small-angle dispersion of a high-energy proton beam, coherent elastic scattering from a nucleus (multiple Coulomb scattering and incoherent pseudoelastic interaction being the others.)

The method is based on a compilation of optical model calculations for the nuclear elastic differential cross section for protons in the center of mass frame for 22 nuclei for $2 \leq \mathrm{A} \leq 242$ and 47 lab momenta over the range $1\ \mathrm{GeV/c} \leq \mathrm{P_{lab}} \leq 50\ \mathrm{GeV/c}$. A formatted data library was derived from the calculated cross sections which provides a representation of the angular distributions as a function of momentum transfer with good interpolation properties over mass and energy. Together with the Monte Carlo sampling method developed for use in MCNP Version 5, the representation accurately reproduces the original optical model calculations over a range of $10^7$.

## II. OPTICAL MODEL CALCULATIONS

The proton-nucleus elastic differential cross sections were calculated for momentum transfers up to 0.85 GeV/c at incident proton laboratory momenta 1 to


*E-mail: rep@lanl.gov



†permanent address: Institute for High Energy Physics, Protvino, Moscow District, Russia

50 GeV/c in the framework of eikonal theory. In this theory, the proton-nucleus phase shifts at a given impact parameter are obtained from integrating the optical potential along a line perpendicular to that impact parameter[2]. At the present stage, we have only used the first-order optical potential which is a convolution between the proton-nucleon scattering amplitudes ($f_{pp}$, $f_{pn}$) and the nuclear matter density. The matter density was derived from the experimental nuclear charge density by removing the proton charge distribution according to the translationally invariant method[3]. We also used the high-energy approximation $f_{pp} = f_{pn}$ and the high-energy parametrization of the amplitudes[4,5]. Without any free parameter, the calculated differential cross sections describe well the existing data, indicating that effects of higher-order optical potential can be expected to be small.

In order to examine the applicability of eikonal theory in light nuclear systems, the p-t and p-$^6$Li elastic differential cross sections given by the eikonal theory were compared with those given by the Glauber theory[6]. For all the energies and momentum transfers considered, the differences are less than 5% for p-t scattering and become negligible for p-$^6$Li scattering. Because the eikonal theory reduces to the Glauber theory when rescatterings of the projectile from the same target nucleon are neglected, the small differences observed in our comparison reveal, therefore, that rescattering effects are very small at high energies.

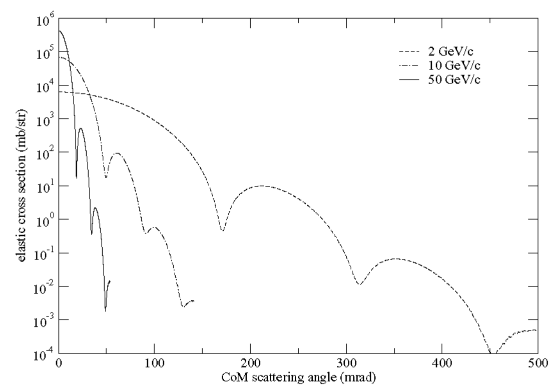


Figure 1: Calculated differential cross section for $p +^{12} C$ at three energies.

Examples of the calculated differential cross sections from which the representation described below is created are shown in figure 1. In this initial effort, the contribution from nuclear-Coulomb interference has been neglected. Proton and neutron densities are each treated as proportional to the nuclear matter densities. In addition, the effects of nuclear deformation are addressed only approximately. Future efforts will include a more detailed representation for the proton and neutron densities and a compilation of elastic differential cross sections for neutrons.

## III. REPRESENTATION FOR THE ANGULAR DISTRIBUTION

For each mass and energy in the data library, the original cross section calculations are represented as a sampling distribution for the dimensionless variable $X$ where

$$X = q/q_1 = 2p\sin(\theta/2)/q_1 \quad (1)$$

for center of mass momentum $p$, momentum transfer $q$, scattering angle $\theta$ and $q_1$, the momentum transfer at the first diffraction minimum. The compiled data library contains a tabulation for $S(X) \sim d\sigma/dX$ normalized to a maximum of unity; $q_1$ is tabulated for the same masses and energies. The same incident energy grid is used for each isotope and the same uniform X-grid applies to all energies for a single isotope. At the present time, the isotopes in the library have either 426 or 851 tabulated points, 171 points for A = 2 and 3.

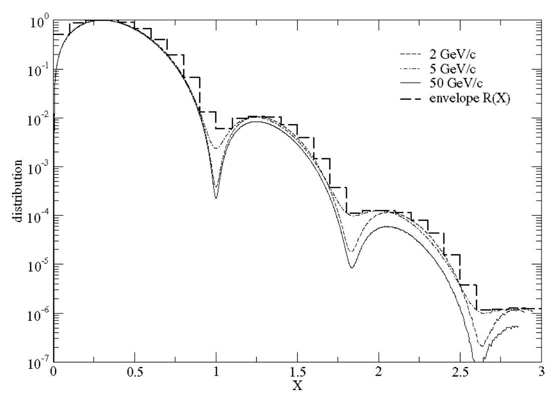


Figure 2: The tabulated function $S(X)$ for $^{12}C$ at three energies and the energy-independent probability distribution $R(X)$.

In addition, an energy independent histogram sampling distribution $R(X)$ is provided for each isotope which provides an "envelope" function: $R(X) \geq S(X)$ for all the energy dependent distributions of that isotope. $R(X)$ is used in the rejection method described below. An example of the functions $S(X)$ and $R(X)$ for $^{12}C$ is shown in figure 2. The representation of $S(X)$ for 5 isotopes at incident momentum 24 GeV/c is shown in figure 3.

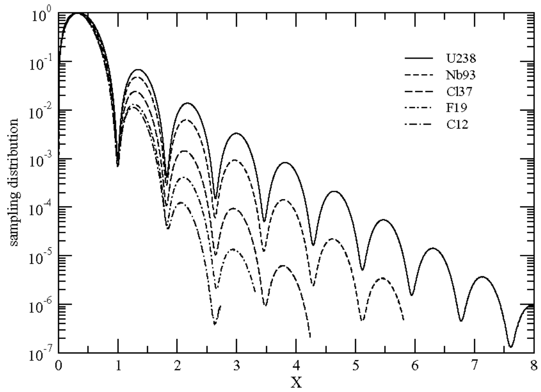


Figure 3: The tabulated function $S(X)$ for 5 (of 22) isotopes at 24 GeV/c.

## IV. MONTE CARLO SAMPLING ALGORITHM

To obtain a center of mass scattering angle, a table energy is selected by random linear interpolation on incident particle kinetic energy energy. A trial value for X is sampled from the energy-independent probability distribution $R(X)$ for the target isotope; for a target *not* in the tabulation, the distribution used is that for the next heavier isotope included. For the selected value of X, the tabulated sampling distribution $S(X)$ is evaluated; for a target *not* in the tabulation, log-log interpolation of the sampling distribution on target mass A is used between adjacent tabulated masses. The sampling efficiency of the method is greater than 80%. As may be noted from figure 3, the representation of the data in the form $S(X)$ greatly minimizes difficulties in interpolating between the tabulated mass values. The variation of $S(X)$ with incident energy for any one mass is well described with the 47 point energy grid. For incident proton momenta above 50 GeV/c, the tabulated data at 50 GeV/c is used.

To complete computation of the center-of-mass scattering angle, the same random selection of an energy tabulation which is applied to obtain $S(X)$ is also applied to obtain $q_1$. Since $1/q_1$ is essentially proportional to an "effective nuclear radius", $1/q_1$ is obtained between tabulated values by linear interpolation in the variable $A^{1/3}$ (see figure 4). The center of mass scattering angle $\theta$ is then evaluated by inversion of equation 1.

To facilitate testing of the methods described above, an alternative processed data library was created containing only alternate target isotopes and alternate energies. In the example shown in figure 5, the elastic differential cross section for protons on $^{93}$Nb at incident kinetic energy 3.17 GeV is shown as (1) the original calculated value, (2) as sampled from the data for $^{93}$Nb at 3.17 GeV, and (3) as sampled by interpolation from data for $^{60}$Ni and $^{133}$Cs at tabulated energies 2.69 GeV and 3.66 GeV. The results are essentially indistinguishable within the statistics for $10^8$ samples.

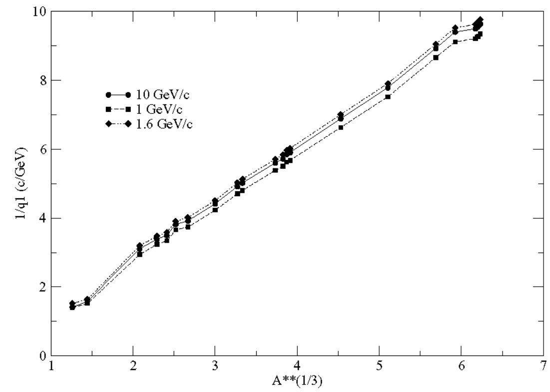


Figure 4: Variation of $1/q_1$ with mass number at three energies.

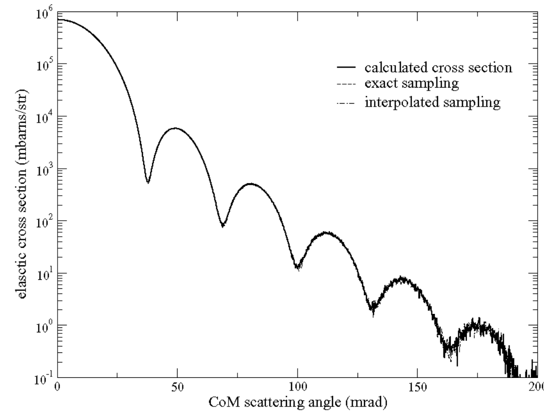


Figure 5: The elastic cross section for protons on $^{93}Nb$ at 3.17 GeV, as originally calculated and as obtained from the sampling algorithm.

## V. VALIDATION

As part of the current effort, a compilation of comparisons with experimental proton scattering data is being prepared, including incident proton momenta from 1.75 GeV/c to 175 GeV/c. Examples of the comparisons are shown in figures 6 and 7. In these figures, three components are shown with the total scattering distribution:

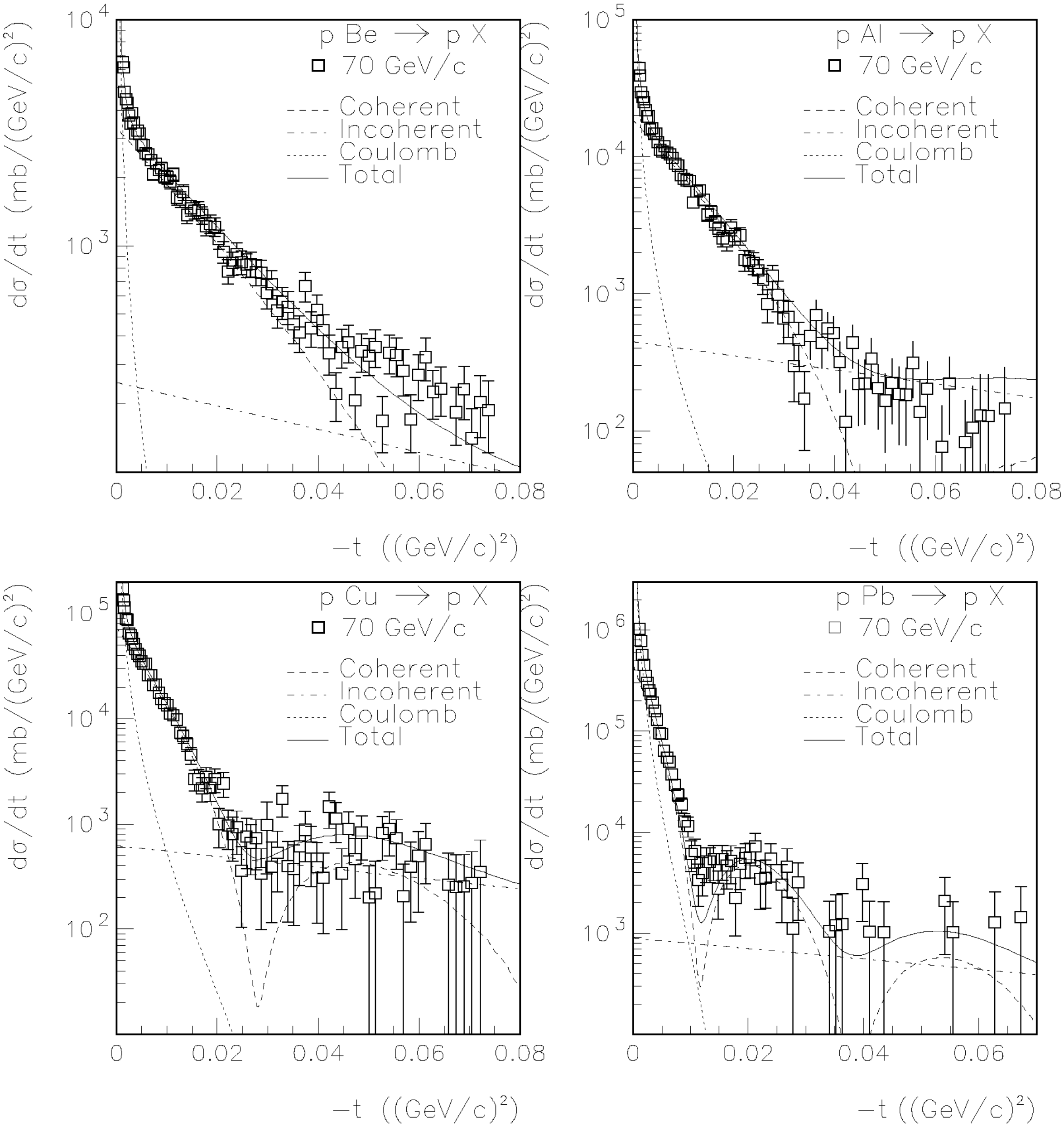


Figure 6: Comparison of model calculations with the data of Schiz et al.[8]

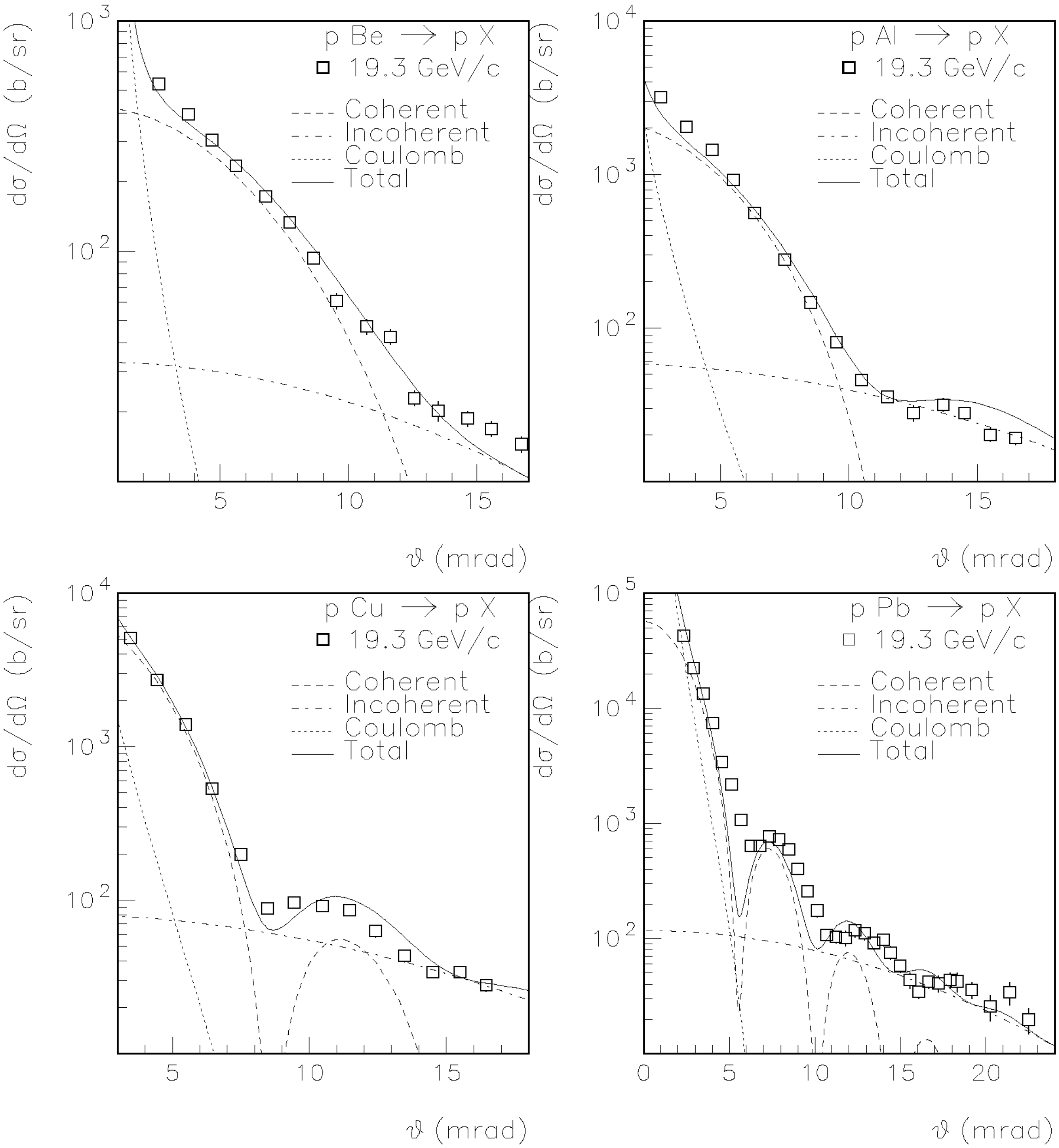


Figure 7: Comparison of model calculations with the data of Bellettini et al.[9]

1. the multiple Coulomb scattering distribution of the uncollided beam;
2. the coherent nuclear elastic scattered component (this work), with multiple Coulomb scattering correction;
3. a simple model of incoherent (quasielastic) proton scattering[7].

An attempt has been made to include the experimental angular resolution, as well as the incident beam angular and momentum spread, in the calculated results. Note that the experimental energy cuts eliminate most diffractive production from the data shown.

The multiple Coulomb scattering calculation is a new formulation[7] being developed for use in MCNP Version 5 in conjunction with the nuclear elastic scattering model. These comparisons show that using a Fermi nuclear form factor (rather than a Gaussian) is important for representing the multiple Coulomb scattering at momentum transfers near the minima for heavy nuclei.

In general, the nuclear elastic scattering representation described here provides a good overall description of the process. In many cases, the modeling does show deeper minima than the experimental data, even after corrections are applied. In the low energies examined, shifts in the location of the minima may perhaps be attributable to the neglect of nuclear-Coulomb interference in the model.

## VI. CONCLUSIONS

The Monte Carlo method described here achieves its objective of providing a highly accurate simulation of proton elastic scattering based on realistic optical model calculations. It is to be hoped that the present work will encourage the development of optical model calculations, including compilations for other incident particles. As additional calculated cross sections for low energies and for neutrons become available, the method will be provided as a general-purpose elastic scattering module; however, it remains to be determined that the representation is equally effective at lower energies.

Validation is only discussed briefly above; when the nuclear elastic scattering model and the multiple Coulomb scattering model are incorporated in MCNP, along with modeling for the incoherent processes, direct simulation of the experimental data will be possible. It will be validation with respect to experiments on macroscopic targets, where multiple Coulomb scattering obscures the details of the scattering process, that will set the priorities for improvements in the nuclear optical model.

## REFERENCES


1. C. L. MORRIS, "Proton Radiography for an Advanced Hydrotest Facility," Los Alamos National Laboratory Report LA-UR-00-5716, Los Alamos, 2000.
2. L. S. RODBERG and R. M. THALER, *Introduction to the Quantum Theory of Scattering*, Academic Press, New York, 1967.
3. L. C. LIU and C. M. SHAKIN, *Nuovo Cimento A* **53**, 142 (1979).
4. K. GOULIANOS, *Phys. Rept.* **3**, 169 (1983).
5. P. H. HANSEN and A. D. KRISCH, *Phys. Rev. D* **15**, 3287 (1977).
6. R. J. GLAUBER and G. MATTHIAE, *Nucl. Phys.B* **21**, 135 (1970).
7. S. STRIGANOV, personal communication.
8. A. SCHIZ et al., *Phys. Rev. D* **21**, 3010 (1980).
9. G. BELLETTINI et al., *Nucl. Phys.* **79**, 609 (1966).